ELSEVIER

A method for measuring endpoint stiffness during multi-joint arm movements

E. Burdet[a,b,c,d,*], R. Osu[c], D. Franklin[b], T. Yoshioka[c], T.E. Milner[b], M. Kawato[c,d]

[a]*Department of Mechanical Engineering, National University of Singapore, 119260 Singapore*
[b]*School of Kinesiology, Simon Fraser University, BC, Canada*
[c]*Kawato Dynamic Brain Project, ERATO, JST, Kyoto, Japan*
[d]*ATR Human Information Processing Research Laboratories, Kyoto, Japan*

Abstract

Current methods for measuring stiffness during human arm movements are either limited to one-joint motions, or lead to systematic errors. The technique presented here enables a simple, accurate and unbiased measurement of endpoint stiffness during multi-joint movements. Using a computer-controlled mechanical interface, the hand is displaced relative to a prediction of the undisturbed trajectory. Stiffness is then computed as the ratio of restoring force to displacement amplitude. Because of the accuracy of the prediction ($<$ 1 cm error after 200 m s) and the quality of the implementation, the movement is not disrupted by the perturbation. This technique requires only $\frac{1}{3}$ as many trials to identify stiffness as the method of Gomi and Kawato (1997, Biological Cybernetics 76, 163–171) and may, therefore, be used to investigate the evolution of stiffness during motor adaptation. © 2000 Elsevier Science Ltd. All rights reserved.

Keywords: Human arm; Voluntary movements; Stiffness measurement; Robotic interface

1. Introduction

Endpoint stiffness of the arm, resulting from the resistance of muscles to a small displacement of the hand, is an important mechanical property of the musculoskeletal system, characterizing resistance to disturbances encountered in the environment (Hogan, 1985). When the hand is perturbed slightly, it tends to return to its original position. Stiffness can be computed as the ratio of restoring force to displacement amplitude.

Using this technique, the features of endpoint stiffness during posture have been investigated extensively (Mussa-Ivaldi et al., 1985; Tsuji et al., 1995; Gomi and Osu, 1998). However, measuring stiffness during multi-joint movements remains a technical challenge. A rigid, powerful mechanical interface with computer-controlled dynamics is also needed to control hand position during movement (Gomi and Kawato, 1997).

Most previous estimates of stiffness during movement have been realized by means of force perturbations. Bennett and others (Bennett et al., 1992; Lacquaniti et al., 1993) have used stochastic force disturbances and measured the resulting change in hand position. This method is relatively straightforward to implement, but results in stiffening of the joints due to muscle co-contraction (Milner, 1993) and can reduce or even abolish the stretch reflex (Stein and Kearney, 1995). For these reasons, Bennett (1993) later employed a displacement relative to the mean undisturbed movement for determining joint stiffness during elbow movements. Although the mechanical interface for displacing the hand must be precisely controlled, only a few trials are needed and data analysis is straightforward (divide force by displacement amplitude).

Force impulses have been used to estimate stiffness during multi-joint movements (Gomi and Kawato, 1997). However, the method suffers from the limitation that a perturbation of the same amplitude, applied at different points in the trajectory or in different directions, will displace the hand by different amounts. This is because limb stiffness depends on joint angles, angular velocity and perturbation direction (Mussa-Ivaldi et al., 1985;

* Correspondence address: Department of Mechanical and Production Engineering, National University of Singapore, 119260, Singapore. Tel.: 65-779-1459;.

E-mail address: e.burdet@ieee.org (E. Burdet).

Gomi and Kawato, 1997; Bennett, 1993). Since the stiffness depends on the displacement amplitude (Shadmehr et al., 1993), bias may result. Furthermore, damping and stiffness must be identified together, so many trials are needed with perturbations in multiple directions.

Consequently, we decided to adapt Bennett's method to study the stiffness of two-joint arm movements. This required consideration of nonlinear limb dynamics, and accurate two-dimensional prediction of where the trajectory would have gone, had there been no perturbation, in order to achieve a constant displacement. For one-joint movements, the mean of past trajectories is an acceptable estimate of the unperturbed trajectory, whereas this is generally not true for multi-joint movements because they are less constrained.

This paper presents the key features of our technique for estimating stiffness during movement: an accurate prediction algorithm for multidimensional trajectories and the implementation of a servo-controlled perturbation during movement. The method is tested in simulations and its efficiency for measuring stiffness without disrupting motion is demonstrated in experiments conducted with two subjects.

2. Methods

Let **q** be the two-dimensional vector with the shoulder and elbow as first and second coordinates, and **x** the corresponding two-dimensional Cartesian hand position vector. Let $\mathbf{F}_a(\mathbf{q(t)},\dot{\mathbf{q}}(t),\ddot{\mathbf{q}}(t))$ be the (endpoint) force required to move the arm along the trajectory $\mathbf{q}(t), 0 \leqslant t \leqslant T$, and let $\mathbf{F}_m(\mathbf{q}(t),\dot{\mathbf{q}}(t),\mathbf{u}(t))$ be the (endpoint) force developed by the muscles activated by **u** to realize this movement. The components of **u** correspond to all the muscles involved in the movement. If there is no interaction with the environment

$$\mathbf{F}_a(\mathbf{q},\dot{\mathbf{q}},\ddot{\mathbf{q}}) \equiv \mathbf{F}_m(\mathbf{q},\dot{\mathbf{q}},\mathbf{u}) \qquad (1)$$

i.e., the sum of the internal forces acting on the musculoskeletal system is **0**. If a force **F** is exerted on the hand (by the mechanical interface), the internal forces are equal to this external force

$$\mathbf{F}_a(\mathbf{q},\dot{\mathbf{q}},\ddot{\mathbf{q}}) - \mathbf{F}_m(\mathbf{q},\dot{\mathbf{q}},\mathbf{u}) \equiv \mathbf{F}. \qquad (2)$$

Let **e** represent a position perturbation in hand Cartesian coordinates with a plateau phase (Fig. 1), during which the following condition is satisfied:

$$\dot{\mathbf{e}} = \ddot{\mathbf{e}} \equiv \mathbf{0}. \qquad (3)$$

By linearizing Eq. (2) about the unperturbed trajectory, we find that the change in force due to the perturbation **e** corresponds to

$$\Delta\mathbf{F} = \frac{\mathrm{d}\mathbf{F}_a}{\mathrm{d}\mathbf{x}}\mathbf{e} + \mathbf{Ke}, \qquad (4)$$
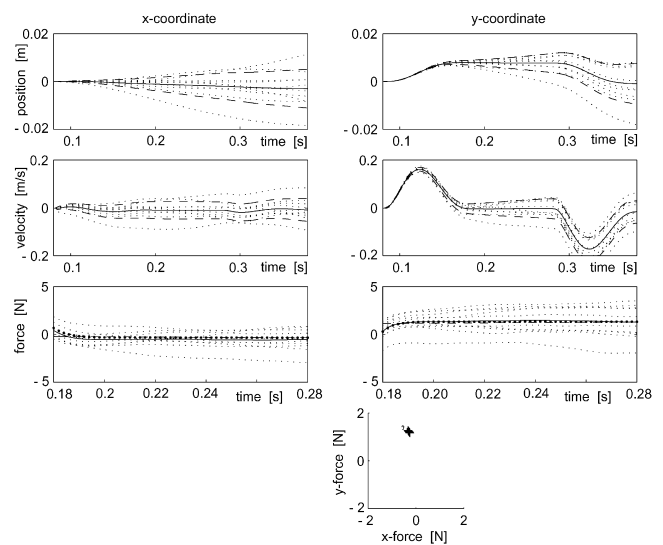

Fig. 1. Elastic force resulting from a position shift in the *y*-direction (movement of Fig. 3). The figure shows the perturbed trajectory minus the undisturbed one. The perturbation was simulated on free movements measured by the interface. The elastic force was computed during the constant phase of the perturbation (note the different time scale of the force plots). In the position and velocity plots, the dotted lines show the error in 10 trials, the solid line their mean, and the dashed lines the mean plus/minus standard deviation. In the force plots, the dotted lines show the estimation resulting from Eq. (4), and the solid lines their mean. The large dots correspond to the force that would result from a perfect trajectory prediction. In the Cartesian force plot, the + correspond to the exact value, and the "," to the estimated value.

where

$$\mathbf{K}(\mathbf{x},\dot{\mathbf{x}},\mathbf{u}) \equiv -\frac{\mathrm{d}\mathbf{F}_m}{\mathrm{d}\mathbf{x}} - \frac{\mathrm{d}\mathbf{F}_m}{\mathrm{d}\mathbf{u}}\frac{\mathrm{d}\mathbf{u}}{\mathrm{d}\mathbf{x}}$$

is the endpoint stiffness. Note that **K** depends on reflexes. $\Delta\mathbf{F}$ corresponds to the mean force measured during perturbed movements minus the mean force required to perform unperturbed movements. We found in simulations that $(\mathrm{d}\mathbf{F}_a/\mathrm{d}\mathbf{x})\mathbf{e}$ can contribute up to 10% of $\Delta\mathbf{F}$ so it cannot be neglected.

Since the trajectory prediction is accurate for only a short time interval (Fig. 1), a good position perturbation must be brief, and the constant position plateau must be reached as quickly as possible. However, a very fast or abrupt transition to the plateau requires the mechanical interface to produce high forces within a brief time, which can lead to vibration. A short transition phase, which miminized vibration (Fig. 1), was achieved by using as servo command a sixth-order polynomial with zero velocity and zero acceleration at the boundaries and zero end jerk (Burdet and Osu, 1999).

The method requires that there be an interval during which the perturbation moves the hand at the velocity of the unperturbed trajectory. To predict the unperturbed trajectory, we noted that trajectories of repeated

movements performed under the same conditions were similar (first panel of Fig. 2). As the velocity profile of any movement was roughly similar to the mean velocity profile of the preceding trials, the shape of the mean profile was used as a template for the current trajectory. The velocity profiles were low-pass filtered at 50 Hz, scaled to produce the same amplitude (in the main movement direction) and truncated at both ends using a 0.03 m s velocity threshold (in the main movement direction) prior to averaging. To avoid distortion of the template due to differences in the times of the peak velocity, the mean was computed independently for the acceleration and deceleration phases. The template velocity was scaled over a range of 11 amplitudes and 11 time shifts, chosen to minimize the prediction error over 20 unperturbed movements. In this way, $11 \times 11 = 121$ candidate
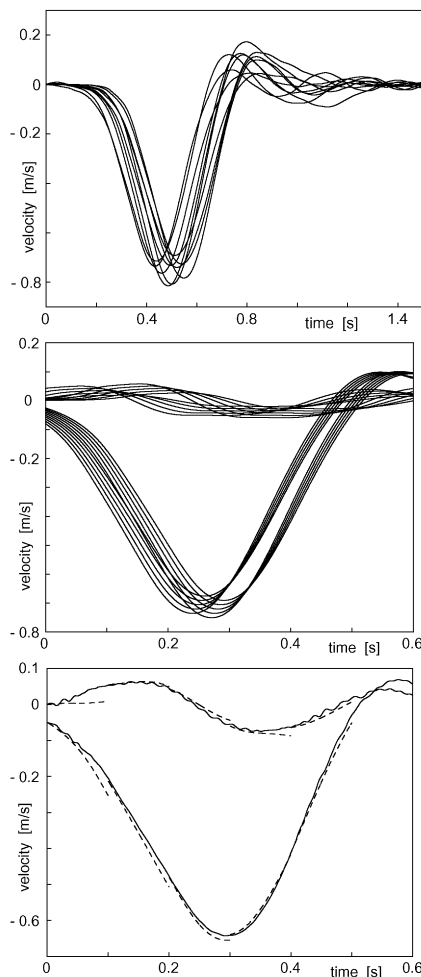

Fig. 2. Steps of the prediction algorithm. The first panel shows the velocity of 10 trials in the main movement direction (measured data). The mean of the 10 velocity measurements is computed, scaled in amplitude and shifted in time to generate 121 velocity profile candidates. Some of these candidates are plotted in the second panel. At any time, the closest candidate can be used to predict the future of the current trajectory. This is illustrated in the third panel. In this graph, the solid lines correspond to the current velocity, and the dashed lines to a prediction carried out every 0.1 s.

velocity profiles were generated (second panel of Fig. 2). The candidate best matching the current trajectory was then selected, and used for predicting the unperturbed trajectory (third panel of Fig. 2). The best match was determined by minimizing the following recursive function once the velocity had crossed a threshold of 0.03 m s:

$$d_{i,k} = (\mathbf{v}_k - \mathbf{w}_{i,k})^2 + \alpha d_{i,k-1}, \tag{5}$$

where $\mathbf{v}_k$ is the velocity of the current time sample k, $\mathbf{w}_{i,k}$ is the ith velocity candidate at time k and $\alpha = 0.94$ is a forgetting factor which limits matching to the last 100 m s. The movement was decomposed parallel and perpendicular to the main movement direction and candidate velocity profiles were selected independently in the two directions.

The template velocity profile, computed as the mean of 10 past movements, was updated after each trial. The standard deviation was computed with the most recent trial replacing the earliest of the 10 stored trials. If the standard deviation was larger than 1.05 times the previous standard deviation, then the most recent trial was excluded, otherwise it was included (Burdet and Osu, 1999).

A horizontal planar parallel manipulator, powered by two DC direct-drive motors controlled at 2 kHz, was used to apply the perturbation (Gomi and Kawato, 1997). The motor shaft angles were measured using optical encoders (409600 pulse/rev) while a force-torque sensor (Nitta Corp. No. 328) mounted on the handle measured the force exerted on the hand to a resolution of 0.06 N.

The speed and acceleration were obtained from the position signal using, respectively, second- and third-order Butterworth filters with a cut-off frequency of 50 Hz, such that differentiation and filtering were realized simultaneously. A feedforward term compensated for the inertia (i.e., the mass matrix multiplied by the acceleration) and the friction, but not for the velocity dependent forces. A relatively small force (< 5 N) was required to perform arm movements (Fig. 3).

The current trajectory was predicted at 1 kHz. The position perturbation was realized using Cartesian PD-trajectory control. The commanded trajectory corresponded to the predicted trajectory plus the perturbation. Note that there was no trajectory control before or after the perturbation. The perturbation had an amplitude of 8 mm and was 300 m s in duration (Fig. 1). Transition phases of up to 100 m s were necessary to minimize vibration. The effect of vibration was avoided by restricting the stiffness identification to a 60 m s interval centered at the midpoint of the plateau phase. Note that the measured stiffness corresponds to a temporal mean over these 60 m s.

The prediction algorithm was tested by simulating the perturbation on free movements measured with the interface. The arm was modeled as a double pendulum with lengths (0.3,0.3) m and masses (1.93,1.52) kg for the
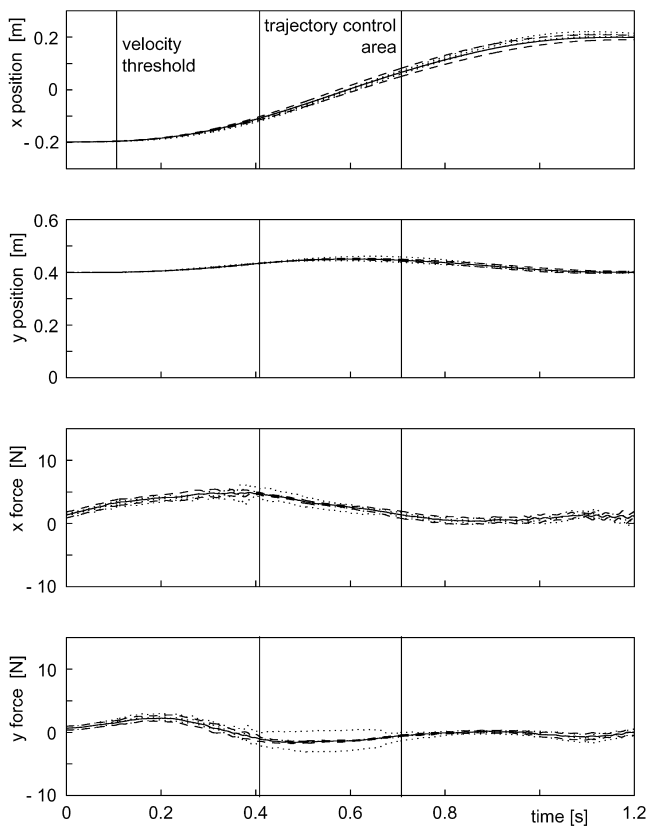
Fig. 3. Position and force measured during movements of amplitude 0.4 m and duration 1 s to the right (Cartesian coordinates relative to the shoulder). The solid and dashed lines correspond, respectively, to the mean of 10 free movements plus/minus standard deviation. The dotted lines are the mean and the mean plus/minus standard deviation of 10 movements with the hand constrained along the prediction of the movement between 0.3 and 0.6 s (relative to a 0.3 m s velocity threshold).
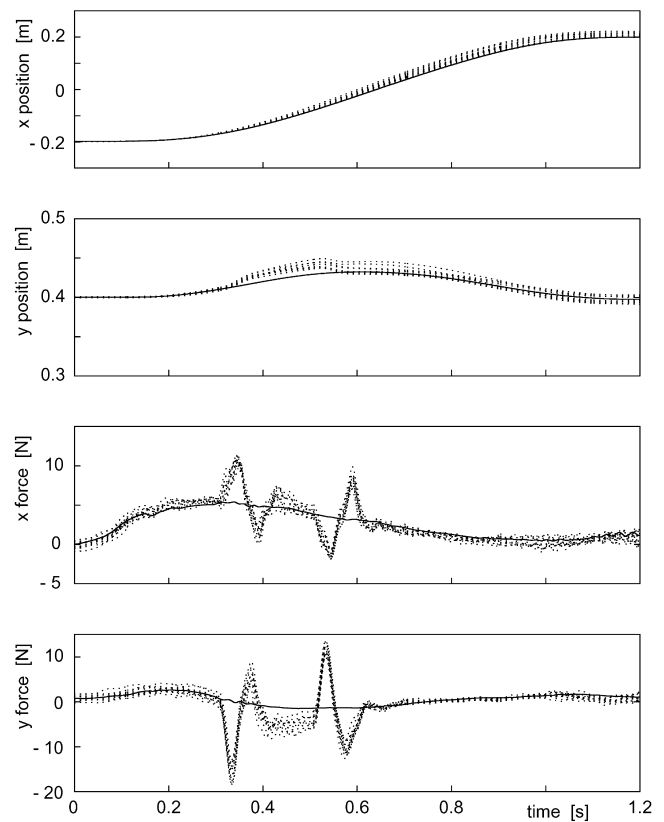

Fig. 4. The same movement than in Fig. 3, with a perturbation of amplitude 8 mm in the y direction. The solid line corresponds to the mean free movement, and the dotted lines to 10 perturbed movements.

upper arm and the lower arm, respectively. The corresponding dynamics $\mathbf{F}_a$ and corrective term $(d\mathbf{F}_a/d\mathbf{x})\mathbf{e}$ were computed numerically. The stiffness matrix $\mathbf{K} \equiv$ [30 10; 10 20] N m was taken from (Gomi and Kawato, 1997).

The implementation was tested on horizontal movements performed by two subjects. The experiments were approved by the institutional ethics committee, and the subjects gave informed consent prior to participation. A perturbation which constrained the hand for the predicted trajectory (0 amplitude) was first tested (Fig. 3), and then a perturbation of amplitude 8 mm (Fig. 4). Finally, stiffness was identified using 40 movements with perturbation directions randomly chosen from the set $\{k(2\pi/8),\ k = 1 \ldots 8\}$ (Burdet et al., 1999).

3. Results

The simulation showed that the prediction error is small (< 1 cm after 200 m s). The prediction error is

sometimes positive, sometimes negative, and distributed symmetrically around the unperturbed velocity (Fig. 1). The mean prediction error is close to 0, and the mean force is close to the force corresponding to perfect trajectory prediction. This indicates that the prediction algorithm and the stiffness estimation are unbiased and accurate.

Tests with a perturbation of amplitude 0 showed that the mechanical interface did not disrupt voluntary movement while driving the hand (Fig. 3). The subjects were unable to detect the perturbation nor did it appear to affect the trajectory importantly. The distance between the means of 10 free movements and of 10 constrained movements was smaller than the standard deviation of the free movements for the position, as well as for the force. Similar consistency was found with the 8 mm amplitude perturbation (Fig. 4). The force was flat, i.e. there was no oscillation, in the 60 m s during which stiffness was identified.

The stiffness values obtained for the two subjects at the midpoint of the movement, listed in Table 1, are of the same order as those of Gomi and Kawato (1997). The deviation is small enough to test hypotheses about the influence of the dynamic environment on stiffness

Table 1
Stiffness measured in two human subjects for the movement of Fig. 3 compared with the approximate value of a typical subject in Gomi and Kawato (1997)[a]

(N m/rad)	Subject ETI	Subject OSU	Gomi97
K_s	40.3 ± 3.0	23.6 ± 3.1	30
K_{se}	21.0 ± 2.3	7.4 ± 2.2	10
K_{es}	12.9 ± 3.0	9.5 ± 3.1	10
K_e	21.3 ± 2.3	14.7 ± 2.2	20

[a] The stiffness, measured in Cartesian space, has been transformed into joint coordinates $K_q \equiv [K_s \ K_{se}; \ K_{es} \ K_e]$ as in McIntyre et al. (1996). The $\pm$ define 95% confidence intervals.

(Burdet et al., 1999). When stiffness was measured on 3 different days, the stiffness values varied by less than 10%.

4. Discussion

The method presented in this paper requires fewer trials to accurately estimate stiffness during movement than methods which have been used previously, including methods based on stochastic perturbations (Bennett et al., 1992; Lacquaniti et al., 1993). Force perturbations, such as those used by Gomi and Kawato (1997), are simpler to implement than our position perturbation. However, both stiffness and damping must be estimated, making the identification more difficult, since damping estimates tend to be inaccurate. Therefore, our technique focused on stiffness identification only. As a consequence, we are able to identify stiffness accurately using only a third as many trials as required by their method.

Although the neuromuscular system is nonlinear, the linear estimation of Eq. (4) is exact if the perturbation amplitude is small enough. In practice, the stiffness value depends on the perturbation amplitude (Shadmehr et al., 1993; Milner and Cloutier, 1993). However, in contrast to the force perturbation method (Gomi and Kawato, 1997), this value is not biased by the perturbation direction.

Because it is not possible to realize a position perturbation briefer than 300 m s, our stiffness estimate, measured between 120 and 180 m s after the beginning of the perturbation, includes a contribution due to reflexes. Future work will investigate the influence of reflexes on the stiffness.

Once the technique introduced in this paper is implemented, it enables a simple and intuitive examination of stiffness during movement: stiffness, which corresponds to the force divided by the (constant) displacement, can be inferred directly from the force plots. This could not be done with methods based on force perturbations (Bennett et al., 1992; Lacquaniti et al., 1993; Gomi and Kawato, 1997). Since our technique is also robust to

gradual changes of the trajectory, it may enable us to examine the evolution of stiffness during motor adaptation.

References

Bennett, D.J., 1993. Torques generated at the human elbow joint in response to constant position errors imposed during voluntary movements. Experimental Brain Research 95, 488–498.

Bennett, D.J., Hollerbach, J.M., Xu, Y., Hunter, I.W., 1992. Time-varying stiffness of human elbow joint during cyclic voluntary movement. Experimental Brain Research 88, 433–442.

Burdet, E., Osu, R., 1999. Development of a new method for identifying muscle stiffness during human arm movements. Report 1-21, Kawato Dynamic Brain Project, ERATO, JST, Japan.

Burdet, E., Osu, R., Franklin, D., Milner, T.E., Kawato, M., 1999. Measuring stiffness during arm movements in various dynamic environments. 1999 ASME Annual Symposium on Haptic Interfaces and Virtual Environments for Teleoperator Systems, Nashville, USA, 421–428.

Gomi, H., Kawato, M., 1997. Human arm stiffness and equilibrium-point trajectory during multijoint movement. Biological Cybernetics 76, 163–171.

Gomi, H., Osu, R., 1998. Task-dependent viscoelasticity of human multijoint arm and its spatial characteristics for interaction with environments. Journal of Neuroscience 18, 8965–8978.

Hogan, N., 1985. The mechanics of multi-joint posture and movement control. Biological Cybernetics 52, 315–331.

Lacquaniti, F., Carrozzo, M., Borghese, N.A., 1993. Time-varying mechanical behavior of multijointed arm in man. Journal of Neurophysiology 69, 1443–1464.

McIntyre, J., Mussa-Ivaldi, F.A., Bizzi, E., 1996. The control of stable postures in the multijoint arm. Experimental Brain Research 110, 248–264.

Milner, T.E., 1993. Dependence of elbow viscoelastic behavior on speed and loading in voluntary movements. Experimental Brain Research 93, 117–180.

Milner, T.E., Cloutier, C., 1993. Compensation for mechanically unstable loading in voluntary wrist movement. Experimental Brain Research 93, 522–532.

Mussa-Ivaldi, F.A., Hogan, N., Bizzi, E., 1985. Neural, mechanical, and geometric factors subserving arm posture in humans. Journal of Neuroscience 5, 2732–2743.

Shadmehr, R., Mussa-Ivaldi, F.A., Bizzi, E., 1993. Postural force fields of the human arm and their role in generating multijoint movements. Journal of Neuroscience 13 (1), 45–62.

Stein, R.B., Kearney, R.E., 1995. Nonlinear behavior of muscles reflexes at the human ankle joint. Journal of Neurophysiology 73, 65–72.

Tsuji, T., Morasso, P.G., Goto, K., Ito, K., 1995. Human hand impedance characteristics during maintained posture. Biological Cybernetics 72, 475–485.